# Increased hurricane frequency near Florida during Younger Dryas Atlantic Meridional Overturning Circulation slowdown

**Michael R. Toomey[1,2], Robert L. Korty[3], Jeffrey P. Donnelly[2], Peter J. van Hengstum[4], and William B. Curry[5]**

[1]*Eastern Geology and Paleoclimate Science Center, U.S. Geological Survey, Reston, Virginia 20192, USA*

[2]*Department of Geology & Geophysics, Woods Hole Oceanographic Institution, Woods Hole, Massachusetts 02543, USA*

[3]*Department of Atmospheric Sciences, Texas A&M University, College Station, Texas 77843, USA*

[4]*Department of Marine Sciences, Texas A&M University at Galveston, Galveston, Texas 77554, USA*

[5]*Bermuda Institute of Ocean Sciences, St. George's GE 01, Bermuda*

**ABSTRACT**

The risk posed by intensification of North Atlantic hurricane activity remains controversial, in part due to a lack of available storm proxy records that extend beyond the relatively stable climates of the late Holocene. Here we present a record of storm-triggered turbidite deposition offshore the Dry Tortugas, south Florida, USA, that spans abrupt transitions in North Atlantic sea-surface temperature and Atlantic Meridional Overturning Circulation (AMOC) during the Younger Dryas (12.9–11.7 k.y. B.P.). Despite potentially hostile conditions for cyclogenesis in the tropical North Atlantic at

this time, our record and numerical experiments suggest that strong hurricanes may have regularly impacted Florida. Less severe surface cooling at mid-latitudes (~20–40°N) than across much of the tropical North Atlantic (~10–20°N) in response to AMOC reduction may best explain strong hurricane activity during the Younger Dryas near the Dry Tortugas and, potentially, along the entire southeastern coast of the United States.

## INTRODUCTION

Reduction in Atlantic Meridional Overturning Circulation (AMOC) during the Younger Dryas (YD), most often attributed to meltwater release during drainage of glacial Lake Agassiz (e.g., Clark et al., 2001 and refs. therein), may have lowered sea-surface temperatures (SSTs) in the North Atlantic (e.g. Schmidt and Lynch-Stieglitz, 2011) and therefore, the potential intensity of tropical cyclones (TCs). However, the environmental controls on TC activity (genesis, track, intensity) are complex, responding not only to changes in local SST but also vertical wind shear and humidity. For instance, Korty et al. (2012) showed a globally heterogeneous response of TC activity to universally colder temperatures in PMIP2 (http://pmip2.lsce.ipsl.fr/) simulations of the Last Glacial Maximum (21 k.y. B.P.). Future, multi-model mean (CMIP5, http://cmip-pcmdi.llnl.gov/index.html), projections, assuming a high emissions scenario, anticipate increased TC potential intensity across much of the tropical North Atlantic by the end of this century (Sobel et al., 2016), but it remains unclear if this would translate into more landfalling intense hurricanes along the basin margins. Historic observations (1947–2015 CE) demonstrate that warm SSTs and low vertical wind shear in the Main Development Region (MDR) (Fig. 1A) have often fostered increased basin-wide TC activity while coinciding with less favorable conditions for storm intensification along the Eastern

Seaboard (Kossin, 2017). No proxy records or comparable modeling experiments of TC activity currently exist for the YD that could be used to test if severe changes in MDR thermodynamic structure, likely to impact cyclone intensity, were counter-balanced by more favorable conditions elsewhere in the basin.

Proxy-based reconstruction of past TC activity using coarse-grained overwash deposits in lower energy back-barrier marshes or lagoons (e.g., Donnelly et al., 2001) has typically been limited to the mid-late Holocene (typically < 5 k.y. B.P.) due to shoreward transgression of these environs in response to deglacial sea-level rise (Bard et al., 2010). However, re-suspension of sediment on continental shelves by storm-induced currents, its subsequent transport offshore and deposition within margin sedimentary sequences could potentially yield much longer records of past TC landfalls. Shanmugam (2008) reviewed observations from modern storms which document bottom water velocities regularly in excess of 1 m $s^{-1}$ on continental shelves and offshore sediment transport. Toomey et al. (2013) found that deposition of coarse-grained layers in an offbank transect of multi-cores (~200–500 m below sea level [mbsl]) from the Bahamas (Fig. 1B) closely tracked the passage of 10 major hurricanes between ~1915 and 1965 CE. Older deposits at that site, thought to reflect increased mid-late Holocene hurricane activity, are consistent with published Caribbean back-barrier overwash records (Toomey et al., 2013 and refs. therein).

Here we use jumbo piston cores (JPCs) from offshore the Dry Tortugas, Florida, that span the YD and early Holocene (EH) (Lynch-Stieglitz et al., 2011), to extend the Bahamas paleo-hurricane reconstruction of Toomey et al. (2013) (located ~400 km east). Florida is in the path of storms tracking out of the eastern Atlantic, western Caribbean and Gulf of Mexico; sedimentary archives there are well positioned to capture changes in North Atlantic cyclogenesis. Together with analysis of general circulation model (GCM) experiments, we address two main questions: (1) how do cooler SSTs and/or AMOC slowdown impact North Atlantic TC activity? (2) Are model-simulated changes in storminess consistent with our proxy-based record of TC landfalls near Florida?

## MATERIALS AND METHODS

The Florida margin (Fig. 1) near the Dry Tortugas Islands (25°N, 83°W) can be divided into four general bathymetric zones: bank-top (~0–60 mbsl), upper-slope (~60–250 mbsl, 2% grade), mid-slope (250–500 mbsl, 5% grade) and toe-of-slope (500–1000 mbsl, 1% grade). An offbank depth transect of cores (JPC25: 494 mbsl; JPC26: 546 mbsl; and JPC59: 358 mbsl) stretching from the upper-slope into the Florida Straits was collected aboard the R/V *Knorr* in January 2002 CE (cruise KNR166-02). Grain size was measured at ~1 cm intervals in these cores, using a Beckman-Coulter (LS13320) laser particle-size analyzer. Bulk mean grain-size data from JPC25, presented in Figure 2A, is archived in the GSA Data Repository[1]. Existing radiocarbon chronology and *Globigerinoides ruber* $\delta^{18}O$ from JPC 26 (Lynch-Stieglitz et al., 2011) was stratigraphically correlated to JPC25/59 using X-ray fluorescence (ITRAX) ln(Ca/Fe), defining the YD and EH boundaries in each core (Fig. DR1). We note, however, that this approach is not aimed at differentiating events occurring in rapid succession and/or short-term changes in local sedimentation rate within the YD or EH.

We also analyzed environmental conditions known to favor TC development and intensification in two segments of the Transient Climate Evolution Experiment (TraCE), a globally coupled ocean-atmosphere-land model simulation performed with Community

Climate System Model version 3.0 (CCSM3) (e.g., Liu et al., 2009). TraCE captures much of the YD SST cooling seen in comparable North Atlantic proxy reconstructions (see Table DR1). We computed TC potential intensity, absolute vorticity, and tropospheric wind shear, which is a measure of tropospheric saturation deficits (see the Data Repository). These metrics can be combined into a genesis potential index (Korty et al., 2012), which measures the combined effects of wind shear, moist thermodynamics, and convection in producing favorable conditions for tropical cyclones to form and intensify. We calculated these variables using monthly TraCE output spanning the middle of the YD (12.5–12.0 k.y. B.P.), during which the North Atlantic was subject to freshwater hosing, and during a later 600-yr segment (10.8–10.2 k.y. B.P.) following establishment of reduced EH meltwater fluxes. Genesis potential was calculated for each month and then summed over June to November of each year; the seasonal totals were averaged over both the YD and EH segments.

## RESULTS AND DISCUSSION

A matrix composed largely of carbonate mud and trace quantities of iron-bearing fines supports coarser-grained biogenic grains in JPC25/26/59. Despite relatively uniform composition, downcore changes in color and iron abundance versus calcium-rich sediments derived from the bank top (Fig. DR1), define tie-points between cores coincident with deglacial flooding of the bank-top (~13 k.y. B.P.), the YD/EH transition (~11.7 k.y. B.P.) and platform submergence (~10 k.y. B.P.). In general, the sediments appear largely structureless, however, evidence of low-density turbidite deposition such as parallel lamina (mm-scale) and sand lenses occur sporadically. Burrows, avoided during sampling, were also occasionally identified by visible changes in sediment structure and/or color. The >63 μm sediment fraction is dominated by benthic foraminifera (primarily miliolids and rotalids), planktonic foraminifera, and occasional pelycopod shell fragments. While we caution that no benthic foraminifera diagnostic of shallow-water origin were observed in the coarsest layers, most of the pelycopod shells were fractured and angular suggesting their taphonomic history included breakage during transport from elsewhere.

We propose that the most likely mechanism for emplacement of coarse-grained material in these cores is entrainment of sediment on the banktop and deposition offshore by turbidites during storms. Grain-size increases downslope (Fig. DR2) and the coarsest beds are poorly sorted relative to background sediments—observations that are inconsistent with winnowing by the Florida Current. Preferential contourite formation during the YD is also unlikely given evidence for greatly reduced AMOC strength at this time (Lynch-Stieglitz et al., 2011; McManus et al., 2004; Fig. 2). Extensive seismic surveying of the southwest Florida margin by Brooks and Holmes (1989) shows depositional units are oriented offbank, not along the path of the Florida Current. We also note higher sedimentation rates during the YD than the ensuing EH, suggesting coarse-grained beds in the YD unit are net-depositional rather than erosional. General agreement between grain-size records from JPC25/26 and JPC59, the latter located ~15 km west along-bank, likely excludes local mass wasting as a viable alternative mechanism for emplacement of coarser-grained units. These sites face no known active margins likely to produce frequent, large, tsunamis nor do they occupy the type of steep continental margin thought to be susceptible to slope failures triggered by distant earthquakes (Johnson et al., 2017). While comparable TC records do not currently exist with which to definitively rule out other local sediment transport mechanisms, given (1) little evidence for contourite formation or tsunami-triggered mass wasting, (2) widespread observations of sediment entrainment on continental shelves during modern storms (Shanmugam, 2008) and (3) sedimentary evidence of density current deposition offbank the Bahamas from historic major hurricanes (Toomey et al., 2013), we argue coarse-grained material in cores JPC25/26/59 is largely derived from storm-triggered turbidites.

Grain-size variability in our cores suggests relatively more frequent high-energy events during the YD with an abrupt transition to finer grained deposition moving into the EH (Fig. 2A; Fig. DR2). For instance, mean grain-size in JPC 25 is 23 ± 4 μm through the YD but drops to 19 ± 2 μm during the EH section (11.7–10.2 k.y. BP). Transgressive drowning of Florida Bank during Meltwater Pulse 1B (MWP1B), ~11.4–11.1 k.y. B.P., limiting entrainment of sediment by storm waves, could provide another explanation for the lack of coarse-grained deposits during the EH; however, recent drilling of drowned reefs offshore Tahiti (Bard et al., 2010, and references therein) indicates a relatively gradual change in the rate of sea-level rise from the YD (~8 mm/yr) to the EH (12 mm/yr), calling into question the existence of MWP1B. Instead, we propose below that sustained AMOC reduction during the YD (McManus et al., 2004) produced environmental conditions that were more hostile to storms across much of the tropical North Atlantic, but locally more favorable near the southeastern U.S.

The spatial pattern of changes in potential intensity (PI) during the YD (Fig. DR3) shows that it was much lower where SSTs fell most dramatically across low latitudes of the tropical Atlantic, but PI was little changed or sometimes higher where SSTs were warmer relative to the remainder of the basin. Near Florida, the seasonal (June–

November) max PI remained high enough to support Category 5 storms throughout the YD and EH (Fig. 3C; YD = 70 m $s^{-1}$, EH = 74 m $s^{-1}$). Vecchi and Soden (2007) showed that PI is strongly related to relative SST rather than to absolute SST: PI is the highest where waters are locally warmer than the regional average. On average, storm season wind shear was higher during the YD than EH across the tropical Atlantic (Fig. DR3), but lower near Florida ($\Delta = -0.3$ m $s^{-1}$) and in the subtropics. In colder atmospheres, a smaller quantity of water vapor is required to saturate an air column. This, in combination with lower shear, yields higher genesis potential (GP in Fig. 3B) with conditions more favorable for tropical cyclones near the Dry Tortugas, outweighing lower absolute local SST (TraCE: YD = 25 °C, EH = 26 °C, comparable to Mg/Ca proxy SST from JPC26; Schmidt and Lynch-Stieglitz, 2011).

In addition to the potential for increased storm activity in the western sub-tropics, genesis potential appears largely unchanged (YD versus EH) in the southern Caribbean (Fig. 3B)—the source region for most major storms tracking near the Dry Tortugas today. Since 1848 CE, 11 of the 12 storms passing the JPC25 core site (≤65 nm radius) as major hurricanes (≥Category 3) formed within or proximal to the Caribbean Sea (Fig. 1A, Knapp et al., 2010), often steered by late season westerlies north/northwest over deep, warm, waters on their way toward Florida. A more southerly mean position of the ITCZ (Haug et al., 2001) and westerlies during the YD could have shifted hurricane tracks toward Florida in late summer when warm Caribbean waters often reach their maximum extent.

Coarse discretization of the TraCE ocean domain (25 vertical levels and ~200–400 km horizontal resolution at these latitudes), however, may limit its sensitivity to thermocline structure and therefore sub-surface warming during episodes of sustained AMOC reduction and/or migrations of the Florida Current itself (~100 km wide)—which may have further augmented favorable TC conditions near our site. Tropical North Atlantic sub-surface temperature is thought to be anti-correlated with AMOC strength (Zhang, 2007) and Mg/Ca temperature estimates from southern Caribbean indicate substantial warming (~3-4 °C) at intermediate depths during the YD (Schmidt et al., 2012). Entrainment of cold water from the thermocline into the surface mixed layer by hurricane-force winds brings colder water to the surface, working as a negative feedback on storm intensity by reducing the transfer of heat to the atmosphere (e.g., Price, 1981). In turn, however, increased hurricane mixing is thought to enhance poleward heat flux (Emanuel, 2001) and, potentially, could have acted as negative feedback on YD high-latitude cooling.

## CONCLUSIONS

Despite cooler local surface temperatures, reconstructed hurricane strikes and GCM experiments suggest relatively strong storm activity along the coast of Florida during the Younger Dryas. While YD conditions for tropical cyclone development appear unfavorable across much of the North Atlantic, the large-scale environment was more conducive for TC genesis and intensification near the southeastern U.S. coast, where SST cooling was less than elsewhere in the basin. Subsurface warming may also have contributed to strong hurricane development near the Dry Tortugas during the YD, motivating future modeling experiments that can better resolve changes in thermocline depth. Complementary storm records along the Eastern Seaboard are also needed to isolate the impact of deglacial sea-level rise on site sensitivity and establish whether increased western North Atlantic hurricane activity is a robust feature of other Pleistocene cold events (i.e., Heinrich) or, possibly, periods of slower AMOC regimes in general.

**ACKNOWLEDGMENTS**

This work was supported by the U. S. Geological Survey Climate and Land Use Change Research and Development Program (Toomey), the Woods Hole Oceanographic Institution Ocean and Climate Change Institute (Toomey) and National Science Foundation grants (OCE-1356708 to Donnelly; 1356509 to van Hengstum). Additional technical support was provided by S. Madsen, R. Sullivan, and E. Roosen. We also thank T. Cronin, M. Robinson, and three anonymous reviewers for their helpful feedback on earlier versions of this manuscript. Any use of trade, firm, or product names is for descriptive purposes only and does not imply endorsement by the U.S. Government.

**REFERENCES CITED**

Bard, E., Hamelin, B., and Delanghe-Sabatier, D., 2010, Deglacial meltwater pulse 1B and Younger Dryas sea levels revisited with boreholes at Tahiti: Science, v. 327, p. 1235–1237, doi:https://doi.org/10.1126/science.1180557.

Brooks, G.R., and Holmes, C.W., 1989, Recent carbonate slope sediments and sedimentary processes bordering a non-rimmed platform: southwest Florida continental margin, *in* Crevello, P.D., et al., eds., Controls on Platform and Basic Development: Society of Economic Paleontologists and Mineralogists Special Publication 44, p. 259–272, doi:https://doi.org/10.2110/pec.89.44.0259.

Clark, P.U., Marshall, S.J., Clarke, G.K., Hostetler, S.W., Licciardi, J.M., and Teller, J.T., 2001, Freshwater forcing of abrupt climate change during the last glaciation: Science, v. 293, p. 283–287, https://doi.org/10.1126/science.1062517.

Donnelly, J.P., Roll, S., Wengren, M., Butler, J., Lederer, R., and Webb, T., 2001, Sedimentary evidence of intense hurricane strikes from New Jersey: Geology, v. 29, p. 615–618, doi:https://doi.org/10.1130/0091-7613(2001)029<0615:SEOIHS>2.0.CO;2.

Emanuel, K., 2001, Contribution of tropical cyclones to meridional heat transport by the oceans: Journal of Geophysical Research, D, Atmospheres, v. 106, D14, p. 14771–14781, https://doi.org/10.1029/2000JD900641.

Haug, G.H., Hughen, K.A., Sigman, D.M., Peterson, L.C., and Röhl, U., 2001, Southward migration of the Intertropical Convergence Zone through the Holocene: Science, v. 293, p. 1304–1308, doi:https://doi.org/10.1126/science.1059725.

Johnson, H.P., Gomberg, J.S., Hautala, S.L., and Salmi, M.S., 2017, Sediment gravity flows triggered by remotely generated earthquake waves: Journal of Geophysical Research: Solid Earth, v. 122, doi:https://doi.org/10.1002/2016JB013689.

Knapp, K.R., Kruk, M.C., Levinson, D.H., Diamond, H.J., and Neumann, C.J., 2010, The International Best Track Archive for Climate Stewardship (IBTrACS): Bulletin of the American Meteorological Society, v. 91, p. 363–376, doi:https://doi.org/10.1175/2009BAMS2755.1.

Korty, R.L., Camargo, S.J., and Galewsky, J., 2012, Tropical cyclone genesis factors in simulations of the Last Glacial Maximum: Journal of Climate, v. 25, p. 4348–4365, doi:https://doi.org/10.1175/JCLI-D-11-00517.1.

Kossin, J.P., 2017, Hurricane intensification along United States coast suppressed during active hurricane periods: Nature, v. 541, p. 390–393, doi:https://doi.org/10.1038/nature20783.

Liu, Z., Otto-Bliesner, B., He, F., Brady, E., Tomas, R., Clark, P., Carlson, A., Lynch-Stieglitz, J., Curry, W., and Brook, E., 2009, Transient simulation of last deglaciation with a new mechanism for Bølling-Allerød warming: Science, v. 325, p. 310–314, doi:https://doi.org/10.1126/science.1171041.

Lynch-Stieglitz, J., Schmidt, M.W., and Curry, W.B., 2011, Evidence from the Florida Straits for Younger Dryas ocean circulation changes: Paleoceanography, v. 26, p. PA1205, doi:https://doi.org/10.1029/2010PA002032.

McManus, J., Francois, R., Gherardi, J.-M., Keigwin, L., and Brown-Leger, S., 2004, Collapse and rapid resumption of Atlantic meridional circulation linked to deglacial climate changes: Nature, v. 428, p. 834–837, doi:https://doi.org/10.1038/nature02494.

Price, J.F., 1981, Upper ocean response to a hurricane: Journal of Physical Oceanography, v. 11, p. 153–175, doi:https://doi.org/10.1175/1520-0485(1981)011<0153:UORTAH>2.0.CO;2.

Schmidt, M.W., Chang, P., Hertzberg, J.E., Them, T.R., Ji, L., and Otto-Bliesner, B.L., 2012, Impact of abrupt deglacial climate change on tropical Atlantic subsurface temperatures: Proceedings of the National Academy of Sciences of the United States of America, v. 109, p. 14348–14352, doi: https://doi.org/10.1073/pnas.1207806109 (erratum available at https://doi.org/10.1073/pnas.1216897109).

Schmidt, M.W., and Lynch-Stieglitz, J., 2011, Florida Straits deglacial temperature and salinity change: Implications for tropical hydrologic cycle variability during the Younger Dryas: Paleoceanography, v. 26, PA4205, doi:https://doi.org/10.1029/2011PA002157.

Shanmugam, G., 2008, The constructive functions of tropical cyclones and tsunamis on deep-water sand deposition during sea level highstand: Implications for petroleum exploration: The American Association of Petroleum Geologists Bulletin, v. 92, p. 443–471, doi:https://doi.org/10.1306/12270707101.

Sobel, A.H., Camargo, S.J., Hall, T.M., Lee, C.-Y., Tippett, M.K., and Wing, A.A., 2016, Human influence on tropical cyclone intensity: Science, v. 353, p. 242–246, https://doi.org/10.1126/science.aaf6574.

Toomey, M.R., Curry, W.B., Donnelly, J.P., and van Hengstum, P.J., 2013, Reconstructing 7000 years of North Atlantic hurricane variability using deep-sea sediment cores from the western Great Bahama Bank: Paleoceanography, v. 28, p. 31–41, doi:https://doi.org/10.1002/palo.20012.

Vecchi, G.A., and Soden, B.J., 2007, Effect of remote sea surface temperature change on tropical cyclone potential intensity: Nature, v. 450, p. 1066–1070, doi:https://doi.org/10.1038/nature06423.

Zhang, R., 2007, Anticorrelated multidecadal variations between surface and subsurface tropical North Atlantic: Geophysical Research Letters, v. 34, L12713, doi:https://doi.org/10.1029/2007GL030225.

## FIGURE CAPTIONS

Figure 1. Site maps. A: Historic North Atlantic hurricane tracks passing within 65 nm of our site at major hurricane strength (96 kts, 1 min maximum sustained wind [MSW]) since 1848 CE (Knapp et al., 2010). White circle pinpoints the Dry Tortugas, abbreviated DT. Location used in Figure 2 proxy reconstructions by dots: red—Vema 12–107 (VM); yellow—Bermuda Rise (BR); light gray—Barbados (BB); dark gray—Cariaco Basin (CB). Tracks noted of major hurricanes that formed in the Caribbean (dark gray) versus one from the eastern North Atlantic (light gray). Background color map was compiled from National Oceanic and Atmospheric Administration (NOAA) monthly satellite-derived ocean heat content data for the 2013–2015 CE storm seasons (Data Repository [see footnote 1]). B: Regional map of southern Florida, northern Caribbean, and Gulf of Mexico. Red arrow shows the generalized path of the Yucatan (YC), Loop and Florida Currents (FC). Location of transect shown in inset C is given by black line from DT to c. Bahamas hurricane reconstruction sites from Toomey et al. (2013) indicated by triangle. Blue shading indicates shallow water areas (<120 mbsl). C: Schematic profile across offbank core transect. Jumbo piston core (JPC) 59 is located ~15 km west of JPC25/26 and projected into line DT-c. Maps were created using Matlab© m_map function suite written by Rich Pawlowicz (University of British Columbia).

Figure 2. Climatic variability across the Younger Dryas/ early Holocene (YD/EH) transition. A: Grain-size record from Florida Straits core KNR166–2 JPC25. Raw data are shown in gray with 50-yr moving average filtered time-series given by blue line. Note broken *y*-axis. B: Mg/Ca paleo-temperature proxy data (red) from core VM12–107 (Schmidt et al., 2012). C: Bermuda Rise (core OCE326-GGC5) $^{231}Pa/^{230}Th$ record of

Atlantic Meridional Overturning Circulation (AMOC) (McManus et al., 2004) (yellow). D: Subsidence corrected relative sea-level records from Barbados (gray) and Tahiti (light blue) adapted from Bard et al. (2010, and references therein). E: Cariaco Basin, Venezuela (Ocean Drilling Program [ODP] Site 1002), %Ti (Haug et al., 2001) (dark gray). Blue and pink shading highlights early Holocene (EH) and Younger Dryas (YD) Transient Climate Evolution Experiment (TraCE) segments, respectively.

Figure 3. Simulated changes in climatic controls on hurricane activity between the Younger Dryas (YD, 12.0–12.5 k.y. B.P.) and early Holocene (EH, 10.2–10.8 k.y. B.P.). Spatial difference in storm season (A) surface temperature and (B) genesis potential index (GPI), averaged for each Transient Climate Evolution Experiment (TraCE) interval. C: Filtered (20 yr) time series of maximum potential intensity near the Dry Tortugas (red) and Barbados (gray) from 13,850 yr B.P. through the EH.

[1]GSA Data Repository item 2017xxx, grain-size data, is available online at http://www.geosociety.org/datarepository/2017/ or on request from editing@geosociety.org.

Figure 1:

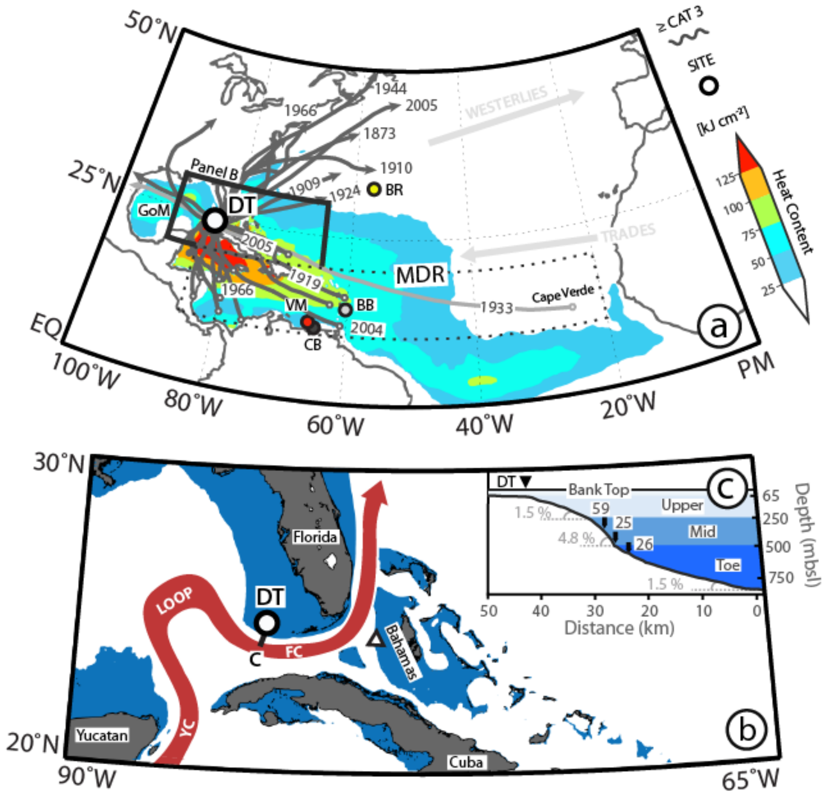

50°N
25°N
EQ
100°W
80°W
60°W
40°W
20°W
PM
≥ CAT 3
SITE
[kJ cm⁻²]
Heat Content
125
100
75
50
25
WESTERLIES
TRADES
1944
2005
1966
1873
1910
1909
1924
BR
Panel B
GoM
DT
2005
1919
1966
MDR
VM
BB
2004
CB
1933
Cape Verde
a
30°N
20°N
90°W
65°W
Florida
DT
LOOP
C
FC
Bahamas
Yucatan
YC
Cuba
b
DT
Bank Top
c
1.5 %
59
25
4.8 %
26
Upper
Mid
Toe
1.5 %
65
250
500
750
Depth (mbsl)
50
40
30
20
10
0
Distance (km)

Figure 2:

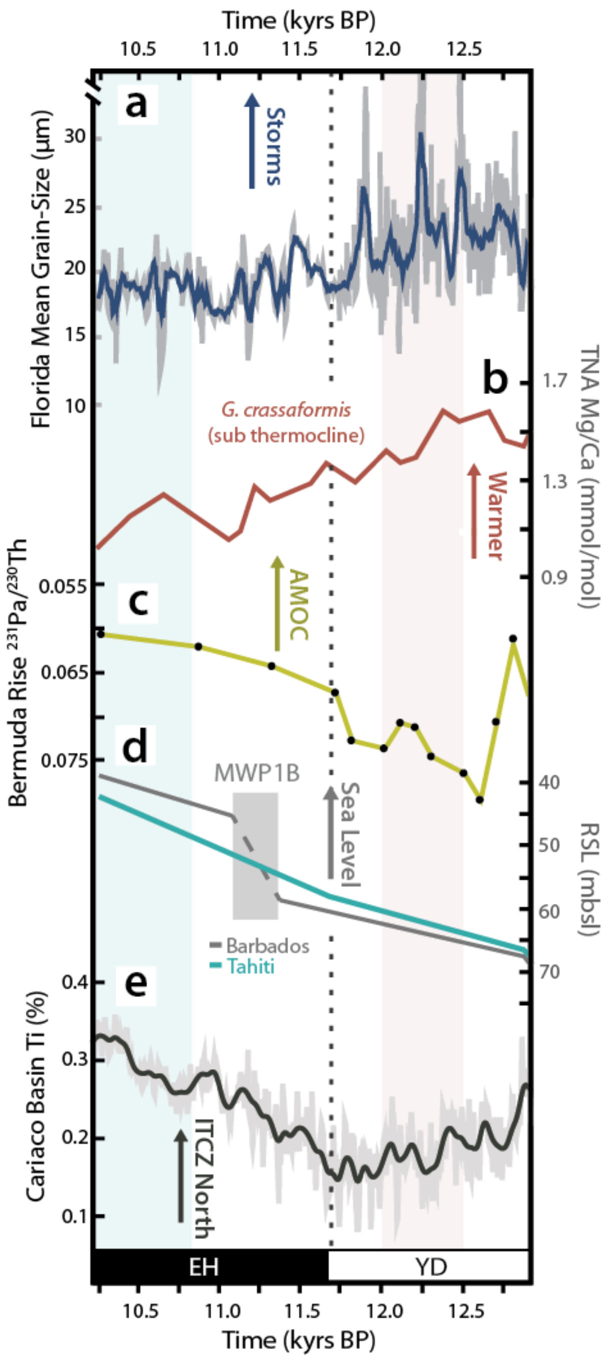
Time (kyrs BP)
10.5
11.0
11.5
12.0
12.5
a
Storms
Florida Mean Grain-Size (µm)
30
25
20
15
10
b
TNA Mg/Ca (mmol/mol)
1.7
1.3
0.9
G. crassaformis
(sub thermocline)
Warmer
c
Bermuda Rise $^{231}Pa/^{230}Th$
0.055
0.065
0.075
AMOC
d
MWP1B
Sea Level
RSL (mbsl)
40
50
60
70
Barbados
Tahiti
e
Cariaco Basin Ti (%)
0.4
0.3
0.2
0.1
ITCZ North
EH
YD
10.5
11.0
11.5
12.0
12.5
Time (kyrs BP)

Figure 3:

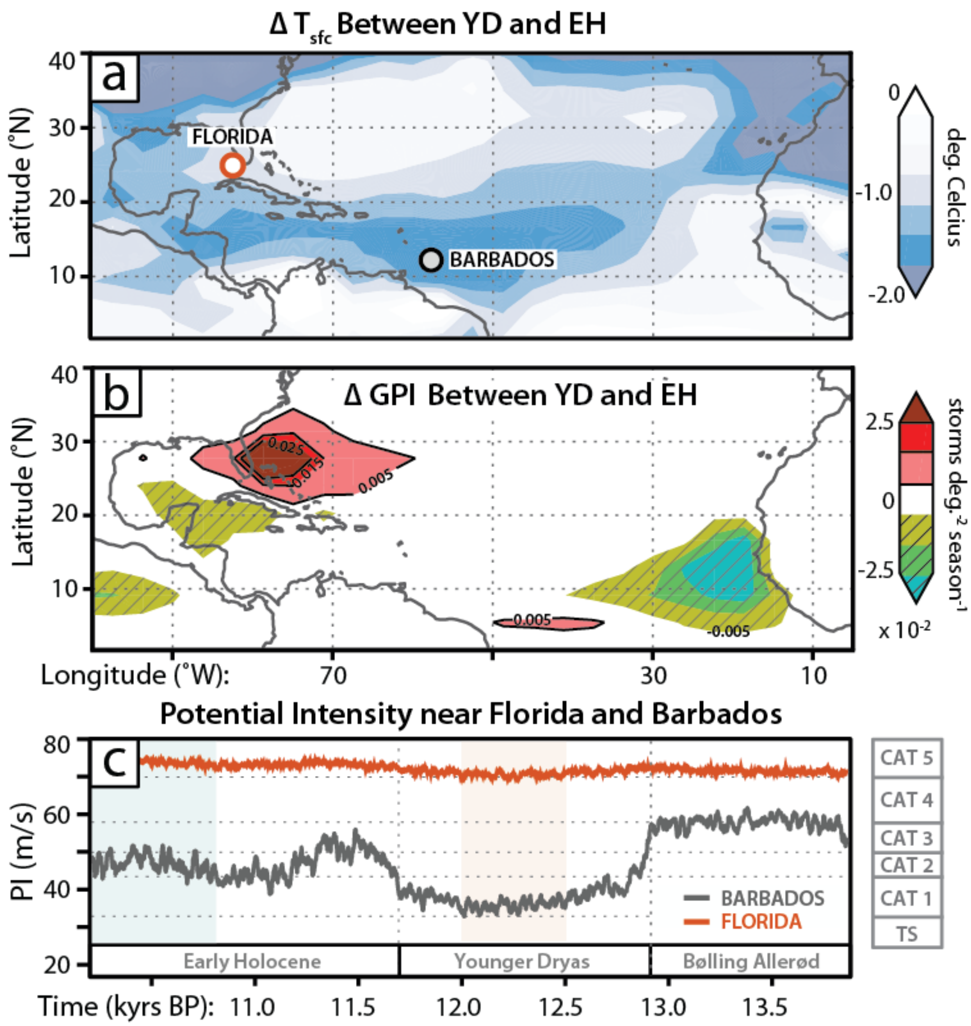
Δ T sfc Between YD and EH
a
Latitude (°N)
40
30
20
10
FLORIDA
BARBADOS
0
-1.0
-2.0
deg. Celcius
b
Δ GPI Between YD and EH
0.025
0.015
0.005
-0.005
2.5
0
-2.5
x 10-2
storms deg.-2 season-1
Longitude (°W):
70
30
10
Potential Intensity near Florida and Barbados
c
PI (m/s)
80
60
40
20
BARBADOS
FLORIDA
CAT 5
CAT 4
CAT 3
CAT 2
CAT 1
TS
Early Holocene
Younger Dryas
Bølling Allerød
Time (kyrs BP):
11.0
11.5
12.0
12.5
13.0
13.5